

DTW+S: Shape-based Comparison of Time-series with Ordered Local Trends

Ajitesh Srivastava

Ming Hsieh Department of Electrical and Computer Engineering

University of Southern California

Los Angeles, USA

ajiteshs@usc.edu

Abstract—Measuring distance or similarity between time-series data is a fundamental aspect of many applications including classification, clustering, and ensembling/alignment. Existing measures may fail to capture similarities among local trends (shapes) and may even produce misleading results. Our goal is to develop a measure that looks for similar trends occurring around similar times and is easily interpretable for researchers in applied domains. This is particularly useful for applications where time-series have a sequence of meaningful local trends that are ordered, such as in epidemics (a surge to an increase to a peak to a decrease). We propose a novel measure, DTW+S, which creates an interpretable “closeness-preserving” matrix representation of the time-series, where each column represents local trends, and then it applies Dynamic Time Warping to compute distances between these matrices. We present a theoretical analysis that supports the choice of this representation. We demonstrate the utility of DTW+S in several tasks. For the clustering of epidemic curves, we show that DTW+S is the only measure able to produce good clustering compared to the baselines. For ensemble building, we propose a combination of DTW+S and barycenter averaging that results in the best preservation of characteristics of the underlying trajectories. We also demonstrate that our approach results in better classification compared to Dynamic Time Warping for a class of datasets, particularly when local trends rather than scale play a decisive role.

I. INTRODUCTION

The distance between two time-series is a fundamental measure used in many applications, including classification, clustering, and evaluation. In classification and clustering, we want two “similar” time-series to have a low distance between them so that they can be grouped together or classified with the same label. In evaluation, the setting could be that we are generating projections (long-term forecasts) of time-series, and retrospectively, we wish to measure how close we are to the ground truth.

While many measures exist for these purposes, including Euclidean distance, correlation, and dynamic time-warping (DTW) [1], the choice of the similarity measure can depend on the domain. Further, existing similarity measures may fail to capture the desired properties of the task at hand, for instance, when we wish to capture the similarity in trends over time. For example, consider the scenario presented in Figure 1a. Two models perform a projection to estimate the time-series given by the ground truth. Model 1 produces a pattern that is similar to the ground truth, while Model 2 produces a flat line. If we use mean absolute error to assess

which model performed better, Model 2 (flat line) will receive a better score. Although Model 1 produces identical trends and correctly predicts the peak timing, it loses to a Model 2 which conveys no information. Now, consider the scenario presented in Figure 1b. Model 1 predicts the exact pattern but it slightly shifted in time. Again, Model 1 – a flat line, produces a lower error. Finally, in Figure 1c, Model 1 predict the overall pattern well, it only misjudges the height of the peaks. Yet, Model 2, a straight line, is considered closer to the ground truth. Some form of a range normalization could have addressed the issue in Figure 1a, and Dynamic Time Warping (DTW) [1], which allows stretching the time dimension to best match two time-series, can address the issue raised in Figure 1b. However, DTW and/or any normalization of scale cannot address the issue presented in Figure 1c.

Our goal is to develop a measure of distance such that two time-series are considered similar if and only if they have a similar sequence of trends and similar trends occur around similar times. This is particularly useful in public health where the time-series may represent meaningful local trends that are ordered, e.g., a surge, followed by an increase, then a peak, and finally a decrease. We define a trend as the local shape of a time-series. Further, we wish this measure to be easily **interpretable** so that it can be adopted by researchers in applied domains, such as epidemiology. To achieve this, we propose a novel distance measure DTW+S that (i) produces a matrix representation where each column encodes local trends, and (ii) uses Dynamic Time Warping on these matrices to compute distances between a pair of time-series. With this measure, we are able to perform better clustering and ensembling [2]–[4] of epidemic curves where local interpretable trends are of interest. While we do not intend to develop a new time-series classification algorithm, we believe a good distance measure should improve a simple distance-based classifier such as k -nearest neighbors [5] on a class of tasks. Therefore, we also demonstrate the success of 1-nearest neighbor using our measure on classification.

Contributions. (1) We prove necessary and sufficient conditions for the shapelet space representation [6] to be closeness-preserving – two local trends are similar if and only if they are mapped to nearby points (Section III-B). (2) We propose a novel distance measure for time-series DTW+S that leverages this representation along with DTW to find if similar trends

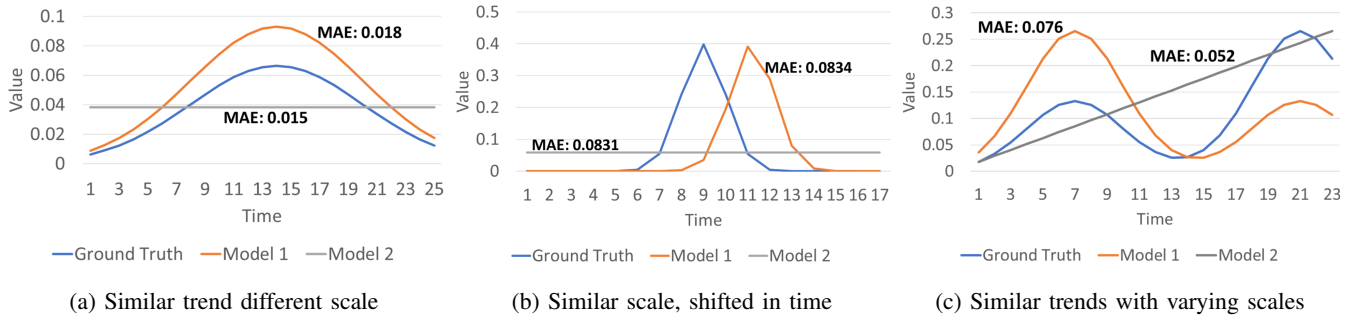


Fig. 1: Simple measures like Mean Absolute Error can be deceiving. In the three scenarios, Model 1 seems to be closer to the Ground truth, but receives a higher distance compared to a straight line.

occur around similar times (Section III-D). (3) We develop an ensembling technique using DTW+S combined with barycenter averaging [7] that can simultaneously summarize time-series in scale and time (Section III-F), and we demonstrate its utility on epidemic curves (Section IV-B). (4) We demonstrate that DTW+S results in more sensible clustering of epidemic curves (Section IV-A). (5) Also, DTW+S outperforms Dynamic Time Warping in classifying time-series on a subset of datasets, particularly, those where local trends play a key role in classification (Section IV-C).

II. RELATED WORK

A. Background

1) *Shapelet Space Representation*: In [6], the idea of the shapelet space representation is introduced to compare short-term forecasts of epidemics. The motivation is to compare the shape of the forecasts rather than exact numerical values. Further, they wish to make the representation interpretable. Each dimension represents the similarity of the vector with one of the chosen shapes of interest, such as an increase (1, 2, 3, 4) and peak (1, 2, 2, 1). These shapes of interest are termed Shapelets.

Definition 1 (Shapelet). A *shapelet* $\mathbf{s} = [s_1, \dots, s_w] \in \mathbb{R}^w$ is a vector that represents a shape of interest.

Definition 2 (Shapelet-space Representation). Given d shapelets $\{\mathbf{s}_1, \dots, \mathbf{s}_d\}$, a *Shapelet-space Representation* of a vector \mathbf{x} is a d -dimensional point $P_x = (p_1, p_2, \dots, p_d)$ capturing the shape of $\mathbf{x} \in \mathbb{R}^w$, where the co-ordinate $p_i = \text{sim}(\mathbf{x}, \mathbf{s}_i)$ for some measure of similarity. The function $f: \mathbb{R}^w \rightarrow \mathbb{R}^d$ is the *Shapelet-space Transformation*.

The similarity function is to be chosen in such a way that two shapes are considered similar if and only if one shape can be approximated by translation and scaling of the other. However, this may cause an issue – when the shape is close to a “flat”, small noise can cause it to become similar to other shapes. It is argued that there is an inherent concept of flatness in the domain of interest. For instance, in influenza when the number of hospitalizations is stable at a very low value, that shape is to be considered flat and not to be considered similar

to any other shape when hospitalizations are higher. Therefore, a desirable property is the following.

Property 1 (Closeness Preservation). *Two vectors have similar representation, if and only if (i) none of the vectors are “almost flat” and one can be approximately obtained by scaling and translating the other, or (ii) both vectors are “almost flat”.*

They propose an approach that first identifies how similar a shape is to what we could consider “flat”, and then updates the similarities of the shape with respect to other shapelets. For some constants $m_0, \beta \geq 0$, define “flatness” as $\phi = \exp(-\beta(m - m_0))$, if $m > m_0$, otherwise $\phi = 1$. Here m is the average absolute slope of the vector \mathbf{x} whose shapelet-space representation is desired, i.e., if $\mathbf{x} = (x_1, x_2, x_3, x_4)$, then $m = (|x_2 - x_1| + |x_3 - x_2| + |x_4 - x_3|)/3$. The constant m_0 enforces that a vector with a very small average absolute slope is considered flat and receives a 0 similarity in all other dimensions. The constant β represents how quickly above the threshold m_0 , the “flatness” should reduce. Now, the co-ordinates of shapelet-space representation are defined as

$$\text{sim}(\mathbf{x}, \mathbf{s}_i) = \begin{cases} 2\phi - 1, & \text{if } \mathbf{s}_i \text{ is “flat”,} \\ (1 - \phi)\text{corr}(\mathbf{x}, \mathbf{s}_i), & \text{otherwise.} \end{cases}$$

It is shown that this definition satisfies Closeness Preservation (Property 1) with w or more shapelets including the “flat” shapelet. We prove that w shapelets are not only sufficient but necessary to satisfy this property (Theorem 2). We use Shapelet-space Representations of moving windows on the given time-series to capture local trends over time.

2) *Dynamic Time Warping*: Dynamic Time Warping (DTW) is a distance measure between two time-series that allows warping (local stretching and compressing) of the time component so that the two time-series are optimally aligned. Given two time-series $\mathbf{a} = [a(1), a(2), \dots]$ and $\mathbf{b} = [b(1), b(2), \dots]$, the objective of DTW is to minimize $\sum_{i \leftrightarrow j} \mathcal{D}(a(i), b(j))$, for some distance measure \mathcal{D} , and where $i \leftrightarrow j$ represents aligning index i of \mathbf{a} with index j of \mathbf{b} . The alignment is done under some constraints – (1) if $a(i)$ and $b(j)$ are aligned then $a(i + 1)$ cannot be aligned with $b(j')$ for some $j' < j$. (2) Every index is present in at least one alignment. (3) The first index of both time-series are aligned

with each other. (4) The last index of both time-series are aligned with each other. Further, a window constraint can be added [8] suggesting that indices i and j can only be aligned if $|i - j| \leq w$, for some non-negative integer w .

3) *Time-series Ensemble*: In applications like epidemic projection, multiple trajectories are generated using different methods or different initializations. Then, an ensemble is created which is then communicated to the public and policy makers [2]. These ensembles are designed to capture the mean value at time t , i.e., for n trajectories $\mathbf{a}_1, \dots, \mathbf{a}_n$, where $\mathbf{a}_i = [a_i(1), \dots, a_i(n)]$ the ensemble is $\bar{a}(t) = \sum_{i=1}^n a_i(t)/n$. As an unintended consequence, informative aspects of individual trajectories may be lost. As an example, consider Figure 2. Two models produce almost identical projections but they are shifted in time, and they have the same peak. The ensemble produces a trajectory that has a peak that is significantly lower and wider than individual models. In public health communication, this can cause a misjudgment of the severity of the epidemic. While the ensemble correctly summarizes the expected outcome at time t , the reader tends to infer other information such as peak timing and severity. Our similarity measure can be used to build ensembles that better preserve the properties of the individual models.

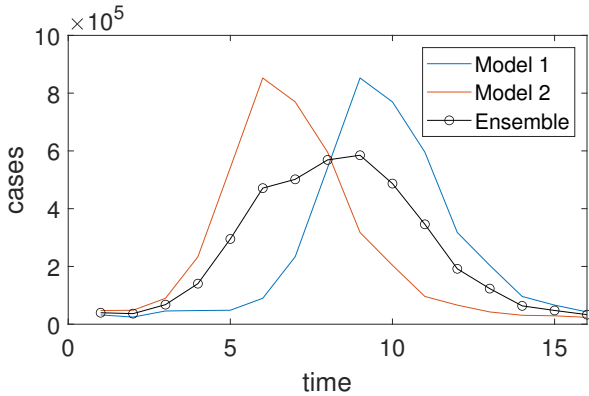


Fig. 2: Failure of the mean ensemble in capturing the properties of individual time-series – much lower peak.

4) *Shapelets*: In time-series literature, “shapelets” have been used to refer to informative motifs that occur in time-series [9]. A feature vector for time-series can then be constructed by similarity of the best matching subsequence of the time-series to these motifs. The motifs are selected based on their representativeness of a class. In contrast, we use the term shapelet as a *pre-determined shape of interest coming from the domain*. We prove that a specific class of shapelet sets and similarity measures is needed to develop a representation to satisfy the closeness-preserving property. We encode all local trends of the time-series into a matrix representation, which is compared using DTW.

B. Related Similarity Measures

While many similarity measures for time-series have been proposed in the literature [10]–[12], the closest work to our

proposed measure DTW+S is ShapeDTW [13]. It was developed as an alignment algorithm that captures point-wise local structures and preferentially aligns similarly-shaped structures. It does so by generating shape descriptors that include the raw sequence, piece-wise aggregation, Discrete Wavelet Transform [14], slopes, and derivatives. A key distinction from our approach is that we utilize a set of shapelets that are shapes of interest in the desired application, and hence our representation is directly interpretable. Further, we present theoretical results on the closeness-preserving characteristics of our approach. While shapeDTW is designed to be general-purpose by constructing a variety of shape descriptors, our approach is particularly designed for applications where the trend is more important than the scale. We later demonstrate that our approach still outperforms shapeDTW for classification on almost half of the 64 datasets considered (Section IV-C).

III. METHODOLOGY

A. Definitions and Overview

First, we define some terms used throughout the text. We start with the idea of a “trend descriptor” that formally defines the idea of assigning arbitrary label (e.g., increase, decrease, peak, etc.) to a part of a time-series. This is intended to emulate a human using categories (implicit or explicit) to interpret a pattern in the time-series. This concept will help us define interpretability of a representation and similarity measure.

Definition 3 (Trend Descriptor). *A trend descriptor is a function \mathcal{L} that maps any vector $\mathbf{x} \in \mathbb{R}^w$ to a label in set L denoting a shape description of \mathbf{x} .*

For instance, a trend descriptor may map any given 4-element vector to one of slow increase, rapid increase, exponential (convex) increase, going towards a peak, going past a peak, rapid decrease, flat, and unknown. Some of these labels may be more similar to each other, e.g., slow and rapid increases are more similar to each other than rapid increase and decrease.

Definition 4 (Local Trend). *For a time-series (a_1, a_2, \dots, a_T) , we define the local trend at location i as $\mathcal{L}(a_i, \dots, a_{i+w-1})$.*

Definition 5 (Interpretable). *We say a representation is interpretable if it is possible to identify the local trends based on the values in each dimension of the representation. We say a distance measure is interpretable if it assigns low distance to two time-series if and only if they have the same local trend.*

Definition 6 (Ordered Local Trend). *A class of time-series has ordered local trends if the similarity between two time-series implies similarity between the sequences of local trends.*

In Figure 1c both orange and blue curves have the same sequence of local trends that can be described as a sequence of increases then peak, followed by a decrease, then a surge, and increase, another peak and decrease. While the gray line is only a sequence of increases. Such characterization is important in understanding and communicating long-term

projections of epidemics as they represent specific events of interest [15], [16].

Our approach consists of two major steps. First, we capture local trends (shapes) of the time-series. To do so, we extend the notion of Shapelet-space Representation to a time-series with a sliding window.

Definition 7 (Shapelet-space Representation - Time-series). *Given a time-series $\mathbf{a} \in \mathbb{R}^{T_1}$, a window w , and a Shapelet-space Transformation $f : \mathbb{R}^w \rightarrow \mathbb{R}^d$, the Shapelet-space Representation of \mathbf{a} is the matrix $\mathbf{A} \in \mathbb{R}^{d \times (T_1 - w + 1)}$ whose i^{th} column is the Shapelet-space Representation of the vector (a_i, \dots, a_{i+w-1}) .*

This matrix encodes how the time-series changes over time in an interpretable manner. Given two time-series, $\mathbf{a} \in \mathbb{R}^{T_1}$ and $\mathbf{b} \in \mathbb{R}^{T_2}$, we first find their Shapelet-space Representations – the matrices $\mathbf{A} \in \mathbb{R}^{d \times (T_1 - w + 1)}$, and $\mathbf{B} \in \mathbb{R}^{d \times (T_2 - w + 1)}$. Each column (of size d) of these matrices is obtained by sliding a w -length window on the respective time-series and obtaining its d -dimensional Shapelet-space Representation (SSR). Figure 3 shows the SSR obtained from a time-series. The SSR is built using four dimensions representing “increase”, “peak”, “surge”, and “flat”. A yellow color represents a high positive value and a blue represents a high negative value (e.g., a negative increase is a decrease). Also note that “surge” and “increase” are similar shapes and hence seem to have a high correlation. The representation tells us that this time series has a sequence of surges/increases leading to a small peak (green in “peak” and “flat”) around time step 5, followed by stability, then increase, leading to a sharp peak (bright yellow around time-step 13), followed by rapid decline (dark blue in “inc”) and then stability (flatness).

Finally, we use Dynamic Time Warping with a suitable window. The distance \mathcal{D} is defined as the Euclidean distance between aligned columns of these matrices. Next, we discuss how to choose a good Shapelet-space Representation.

B. Choosing the Shapelet-Space

While Srivastava et. al. provide some indication of how to choose the set of shapelets, they only prove that for vectors with w elements, w shapelets are sufficient. While one may choose more number of shapelets, e.g., one for each trend descriptor in mind, having a large number (d) of shapelets also impacts the space and time complexities as both scale linearly with d . What is the minimum number of shapelets needed? Here, we show that w shapelets are not only sufficient but also necessary to satisfy the closeness-preserving property. Let $f : \mathbb{R}^w \rightarrow \mathbb{R}^d$ be a shapelet transformation obtained by a set of linearly independent vectors $\mathbf{s}_1, \dots, \mathbf{s}_{d-1}$ and the flat vector \mathbf{s}_0 . Consider two vectors \mathbf{x} and \mathbf{y} of length w . Suppose \mathbf{x}' and \mathbf{y}' represent the corresponding normalized vectors obtained as: $\mathbf{x}' = \frac{\mathbf{x} - \mu_{\mathbf{x}}}{\|\mathbf{x}\|}$ and $\mathbf{y}' = \frac{\mathbf{y} - \mu_{\mathbf{y}}}{\|\mathbf{y}\|}$, where $\mu_{\mathbf{x}}$ and $\mu_{\mathbf{y}}$ are the mean of elements in the vectors \mathbf{x} and \mathbf{y} , respectively.

Theorem 1. *Property 1 is satisfied with any set of $w - 1$ linearly independent shapelets and the “flat” shapelet, i.e.,*

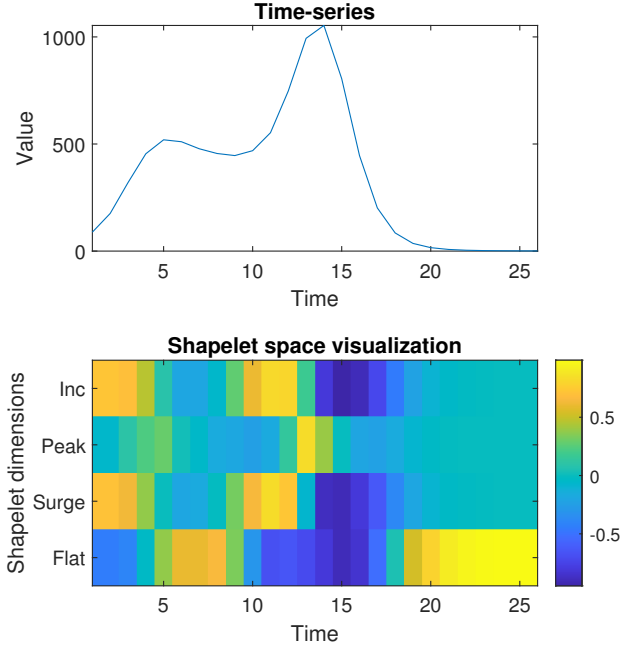


Fig. 3: Shapelet-space Representation of a time-series.

with this choice $\|f(\mathbf{x}) - f(\mathbf{y})\| \leq \epsilon$ iff (i) both \mathbf{x} and \mathbf{y} are “almost” flat, or (ii) $\|\mathbf{x}' - \mathbf{y}'\| \leq \delta$, for some small ϵ and δ .

Proof. Suppose $\|f(\mathbf{x}) - f(\mathbf{y})\| \leq \epsilon$.

If both vectors are approximately flat then, without loss of generality, we can assume that $\phi_x \geq \phi_y \geq 1 - \epsilon$, for some small ϵ . Then, along the flat dimension, $|2(\phi_x - 1) - 2(\phi_y - 1)|^2 \leq 4(1 - (1 - \epsilon))^2 \leq 4\epsilon^2$. And, along any other dimension,

$$\begin{aligned} |(1 - \phi_x)\mathbf{s}'^T \mathbf{x}' - (1 - \phi_y)\mathbf{s}'^T \mathbf{y}'|^2 &\leq |(1 - \phi_y) \cdot 1 - (1 - \phi_x) \cdot (-1)|^2 \\ &= |2 - (\phi_x + \phi_y)|^2 \leq |2 - 2(1 - \epsilon)|^2 \leq 4\epsilon^2. \end{aligned}$$

So, $\|f(\mathbf{x}) - f(\mathbf{y})\|^2 \leq 4(w - 1)\epsilon^2 + 4\epsilon = 4w\epsilon^2 = \epsilon^2$, where $\epsilon = \epsilon/(2\sqrt{w})$.

Now, suppose that both vectors are not “almost” flat and $\phi_x \geq \phi_y$. Let $\epsilon^2 = \sum_i \epsilon_i^2$, where ϵ_i is the difference in the i^{th} dimension of $f(\mathbf{x}) - f(\mathbf{y})$. Then, along the dimension corresponding to \mathbf{s}_0 :

$$|(2\phi_x - 1) - (2\phi_y - 1)| \leq \epsilon_0 \implies \phi_x \leq \phi_y + \epsilon_0/2. \quad (1)$$

Now, since $\phi_y \leq \phi_x \leq \phi_y + \epsilon_0/2$, then a small ϕ_y would imply that ϕ_x is also small. Therefore, both ϕ_x and ϕ_y are not small.

Now, along any other dimension i ,

$$\begin{aligned} \epsilon_i &= |(1 - \phi_x)\mathbf{s}'^T \mathbf{x}' - (1 - \phi_y)\mathbf{s}'^T \mathbf{y}'| \\ &= |(1 - \phi_x)\mathbf{s}'^T (\mathbf{x}' - \mathbf{y}') + (1 - \phi_x)\mathbf{s}'^T \mathbf{y}' - (1 - \phi_y)\mathbf{s}'^T \mathbf{y}'| \\ &= |(1 - \phi_x)\mathbf{s}'^T (\mathbf{x}' - \mathbf{y}') + (\phi_y - \phi_x)\mathbf{s}'^T \mathbf{y}'| \\ &\geq |(1 - \phi_x)\mathbf{s}'^T (\mathbf{x}' - \mathbf{y}')| - \epsilon_0/2. \end{aligned}$$

And thus,

$$\begin{aligned} |(1 - \phi_x) \mathbf{s}'^T (\mathbf{x}' - \mathbf{y}')| &\leq \epsilon_i + \epsilon_0/2 \\ \implies |\mathbf{s}'^T (\mathbf{x}' - \mathbf{y}')| &\leq \frac{\epsilon_i + \epsilon_0/2}{1 - \phi_x}, \forall i \in \{1 \dots w - 1\}. \end{aligned} \quad (2)$$

Additionally, we note that due to the normalization,

$$\mathbf{1}^T \mathbf{y}' = \mathbf{1}^T \mathbf{x}' = 0 \implies \mathbf{1}^T (\mathbf{y}' - \mathbf{x}') = 0, \quad (3)$$

where $\mathbf{1}$ is the vector of all ones. Now consider a matrix C_w with w rows whose i^{th} row is given by \mathbf{s}'_i , for $i \leq w - 1$ and w^{th} row is $\mathbf{1}$.

$$C_w (\mathbf{x}' - \mathbf{y}') = \mathbf{e}, \quad (4)$$

where i^{th} row of \mathbf{e} for $i < w$ is given by some $|e_i| \leq \frac{\epsilon_i + \epsilon_0/2}{1 - \phi_x}$ and the w^{th} entry is 0. We show that $\mathbf{1}$ is linearly independent of all the $w - 1$ other rows. Recall that \mathbf{s}'_i are all μ -normalized, and so $\mathbf{1}^T \mathbf{s}'_i = 0, \forall i$. Therefore, all w rows of C_w are linearly independent, i.e., C_w is full rank and invertible. So, we have

$$\begin{aligned} \mathbf{x}' - \mathbf{y}' = C_w^{-1} \mathbf{e} &\implies \|\mathbf{x}' - \mathbf{y}'\| = \|C_w^{-1} \mathbf{e}\| \\ &\leq \|C_w^{-1}\| \|\mathbf{e}\| \leq \|C_w^{-1}\| \sqrt{\sum_{i=1}^{w-1} \left(\frac{\epsilon_i + \epsilon_0/2}{1 - \phi_x} \right)^2} = \delta, \end{aligned} \quad (5)$$

which is small for finite $\|C_w^{-1}\|$ and small $\epsilon_i, \forall i \geq 0$. \square

Theorem 2. *At least $w - 1$ linearly independent shapelets are necessary with the “flat” shapelet to satisfy property 1.*

Proof. We will show that choosing $w - 2$ independent shapelets results in at least one $\mathbf{y} \neq \mathbf{x}$, such that $f(\mathbf{x}) = f(\mathbf{y})$ and none of them are flat, i.e., $\phi_x, \phi_y < 1$. Since the vectors are equal across all dimensions, $2\phi_x - 1 = 2\phi_y - 1 \implies \phi_x = \phi_y$. Therefore, for all other dimensions:

$$(1 - \phi_x) \mathbf{s}'_i^T \mathbf{x}' = (1 - \phi_y) \mathbf{s}'_i^T \mathbf{y}' \implies \mathbf{s}'_i^T (\mathbf{y}' - \mathbf{x}') = 0. \quad (6)$$

Consider the matrix C_{w-1} whose i^{th} row for $i \leq w - 2$ is \mathbf{s}'_i and $(w - 1)^{\text{th}}$ row is $\mathbf{1}$. Since all of its rows are independent, its rank is $w - 1$. Using rank-nullity theorem [17], its nullity is 1. Therefore, \exists a vector $\mathbf{u} \in \mathbb{R}^w$, with $\|\mathbf{u}\| = 1$ such that,

$$\mathbf{y}' - \mathbf{x}' = p\mathbf{u} \implies \mathbf{y}' = \mathbf{x}' - p\mathbf{u} \quad (7)$$

We will prove that there exists a solution to the above other than the trivial solution $p = 0$. First, taking the square of the norm of both sides of Equation 7

$$\begin{aligned} \|\mathbf{y}'\|^2 = \|\mathbf{x}' + p\mathbf{u}\|^2 &\implies 1 = \|\mathbf{x}'\|^2 + p^2 \|\mathbf{u}\|^2 + 2p\mathbf{u}^T \mathbf{x}' \\ \implies 1 = 1 + p(p + 2\mathbf{x}'^T \mathbf{u}') &\implies p = 0 \text{ or } p = -2\mathbf{u}^T \mathbf{x}'. \end{aligned} \quad (8)$$

Therefore, for any given \mathbf{x}' , if $\mathbf{u}^T \mathbf{x}' \neq 0$, there exists $\mathbf{y}' \neq \mathbf{x}'$ which has the same shapelet space representation. In fact, there are infinitely many such \mathbf{x}' for which this holds. As a demonstration, pick any \mathbf{x}' which is linearly independent with

all the $w - 1$ rows in C_{w-1} and is not a zero vector. To see that this choice works, note that if $\mathbf{x}'^T \mathbf{u} = 0$, then the nullity of the matrix C'_w formed by appending \mathbf{x}' as a row to matrix C_{w-1} is 1 (i.e., \mathbf{u} spans the null space of C_w). However, as all w rows of C'_w are linearly independent, its rank is w , which violates the rank-nullity theorem. As a result, there exists a $\mathbf{y}' \neq \mathbf{x}'$ such that $f(\mathbf{x}') = f(\mathbf{y}')$. \square

Discriminating any \mathcal{L} : Due to the closeness preserving property, it follows that with w shapelets as described above, we can distinguish between any two local trends taken from an arbitrary choice of scale-free trend descriptor \mathcal{L} . By scale-free we mean a trend descriptor that does not distinguish based on scale, e.g., “high increase” vs “very high increase”. On the other hand, it should be noted that we do not completely ignore the scale information. The flat dimension can be rewritten as $\text{sim}(\mathbf{x}, \text{flat}) = 2\phi - 1 = 2\exp(-\beta m)$, choosing $m_0 = 0$. Given, the value in the flat dimension, we can uniquely find the average absolute slope m and thus we are able to discriminate scale-based trend descriptors as well. Therefore, by choosing the w shapelets appropriately, we can discriminate any two local trends taken from an arbitrary choice of \mathcal{L} .

C. Algorithm

Here we present the pseudocode for DTW+S. Algorithm 1 implements our approach. It calls the function *TimeSeriesShape* to compute SSR of the input time-series, which is presented in Algorithm 2. The function *ShapeletSpaceTransform* uses the similarity and shapelets described in the paper.

Algorithm 1 Dynamic time warping with shapes

```

procedure DTW+S(a, b, S,  $\tau$ )
  A = TimeSeriesShape(a, S)
  B = TimeSeriesShape(b, S)
  return DTW(A, B,  $\tau$ )
end procedure

```

Algorithm 2 Extracting shapelet space representation of time-series using a moving window

```

procedure TIMESERIESSHAPE(a, S)
   $w \leftarrow$  length of each shapelet in S
   $T \leftarrow$  length of the time-series a
  for dot = 1 to  $T - w + 1$ 
    A[:,  $t$ ] = ShapeletSpaceTransform(a[ $i : i + w - 1$ ], S)
     $\triangleright$  Take a window of length  $w$  and transform it into
    the shapelet space
  end for
end procedure

```

D. Time-series Similarity: DTW+S

Recall that our goal is to consider two time-series similar if they have similar shapes around the same time, but not necessarily *at* the same time. To allow this, we use Dynamic Time Warping where the distance between aligning column

i with column j is given by the square of the Euclidean distance between the i^{th} column of \mathbf{A} and j^{th} column of \mathbf{B} , i.e., $\|\mathbf{A}[:, i] - \mathbf{B}[:, j]\|^2$. Figure 11 provides a visualization of SSR matrices. Details of the interpretation are provided in Section V. The choice of warping window τ depends on the application. For a classification task, it can be treated as a hyper-parameter and identified through validation on a held-out set. For epidemics, suppose, two models generate projections under the same assumptions, they may be predicting multiple peaks. Far-away peaks may refer to different events (e.g., two different variants causing two waves). However, peaks that occur 4-5 weeks apart across models may be referring to the same event. Therefore, $\tau = 5$ weeks would be a reasonable choice.

E. Clustering and Classification

We can use DTW+S to cluster time-series with any clustering or classification algorithm that allows customizable distance measures. As a demonstration, we use agglomeration clustering [18] on the distance matrix where each entry $\mathcal{D}(\mathbf{a}_i, \mathbf{a}_{i'})$ is the DTW+S distance of time-series i_1 and i_2 . The algorithm starts with each time-series as its own cluster, and then recursively merges clusters greedily based on the distances. We use Silhouette Coefficient [19] to decide the optimal number of clusters. For classification, we use the 1-nearest neighbor method [5]. The choice was made so that the decisive factor in correct classification is the distance measure. That is, two time-series that are closest to each other belong to the same class. This is also a popular way of evaluating distance measures between time-series [20].

F. Ensemble Generation

The existing ensemble methods are designed to aggregate individual projections over time, thus measuring the scale (e.g., number of hospitalizations) at time t . They are not designed to aggregate when will an event (e.g., a peak) take place. However, a viewer tends to interpret both the scale and timing from the ensemble plot. We are interested in – given n time-series, $\mathbf{a}_i = [a_i(1), a_i(2), \dots, a_i(T)]$, $i \in \{1, \dots, n\}$, find an “ensemble” time-series that captures the aggregate behavior in both time and scale. To address this, we assume that each trajectory tries to estimate a sequence of latent “events”. With this perspective, for some sequence of event e_1, e_2, \dots , a time-series captures the timing of e_j and its scale. Therefore, the time-series can be interpreted as $\mathbf{a}_i = [(t_i(e_1), a_i(e_1)), (t_i(e_2), a_i(e_2)), \dots]$. For any given event e_j , the aggregate time-series can be obtained by averaging both the timing and the severity dimensions of the individual time-series:

$$(\bar{t}(e_j), \bar{a}(e_j)) = \left(\frac{\sum_i t_i(e_j)}{n}, \frac{\sum_i a_i(e_j)}{n} \right) \quad (9)$$

However, we do not observe these “events” explicitly. We define an event to be reflected in the time-series by a local trend. When two time-series are aligned by DTW+S, each alignment corresponds to an event. Formally, in the shapelet

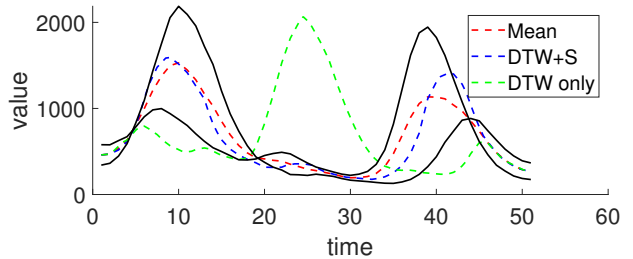


Fig. 4: Applying mean, DTW, and DTW+S to develop ensemble of two time-series.

space representation \mathbf{A} and \mathbf{B} , if columns τ_1 and τ_2 are aligned, then the local trend at time $[\tau_1, \tau_1 + w - 1]$ in time-series \mathbf{a} and that at time $[\tau_2, \tau_2 + w - 1]$ in time-series \mathbf{b} are defined to be corresponding to the same “event”. Suppose we use DTW+S to align n projections. Then, each projection i contributes one point $(t_i(j), a_i(t_j))$ for each alignment j . This results in a set of points, one for each alignment j , using Equation 9. Finally, if desired, we can interpolate these points to estimate the value of $\bar{a}(t)$ for $t \in \{1, 2, \dots, T\}$. Note that this approach is based on the following assumptions. First, each time-series has a similar sequence of shapes but may differ in timing and severity/scale. Second, the interpolation assumes smoothness in the desired ensemble.

Figure 4 demonstrates this approach for two time-series (in black solid line) that have two peaks each with different scales. We compare our approach against the mean ensemble and DTW (without SSR). Note that the mean ensemble results in a small second peak which is closer to the smaller peak among the input time-series. Further, its timing is biased towards the larger peak. The DTW ensemble results in one large peak by aggregating scale and timing of the first peak of one and the second peak of the other time-series. The DTW+S ensemble results in two peaks as expected, where each peak correctly averages the corresponding timing and scale of the input time-series.

While similar aggregation has been discussed in the literature [7], [21], two key differences exist. First, our application is motivated by visual interpretation of “events”, such as when the epidemic peaks. Second, our approach uses an interpretable shape-based measure instead of directly using the Euclidean distance on time-series. This allows us to define an “event”.

Optimally aligning multiple time-series is NP-Hard with some polynomial time approximation algorithms including DTW Barycenter Averaging [7]. In this approach, the initial ‘base’ time-series is selected as the time-series among the set of trajectories that has the lowest distance from other trajectories. Then, in each iteration, we compute the pairwise alignment of all time-series with respect to the base time-series and the result becomes the new ‘base’ time-series. The alignment is traditionally computed using DTW, which we replace with DTW+S. We demonstrate that the DTW+S based Barycenter Averaging is better at capturing the properties of the constituent trajectories (Section IV-B).

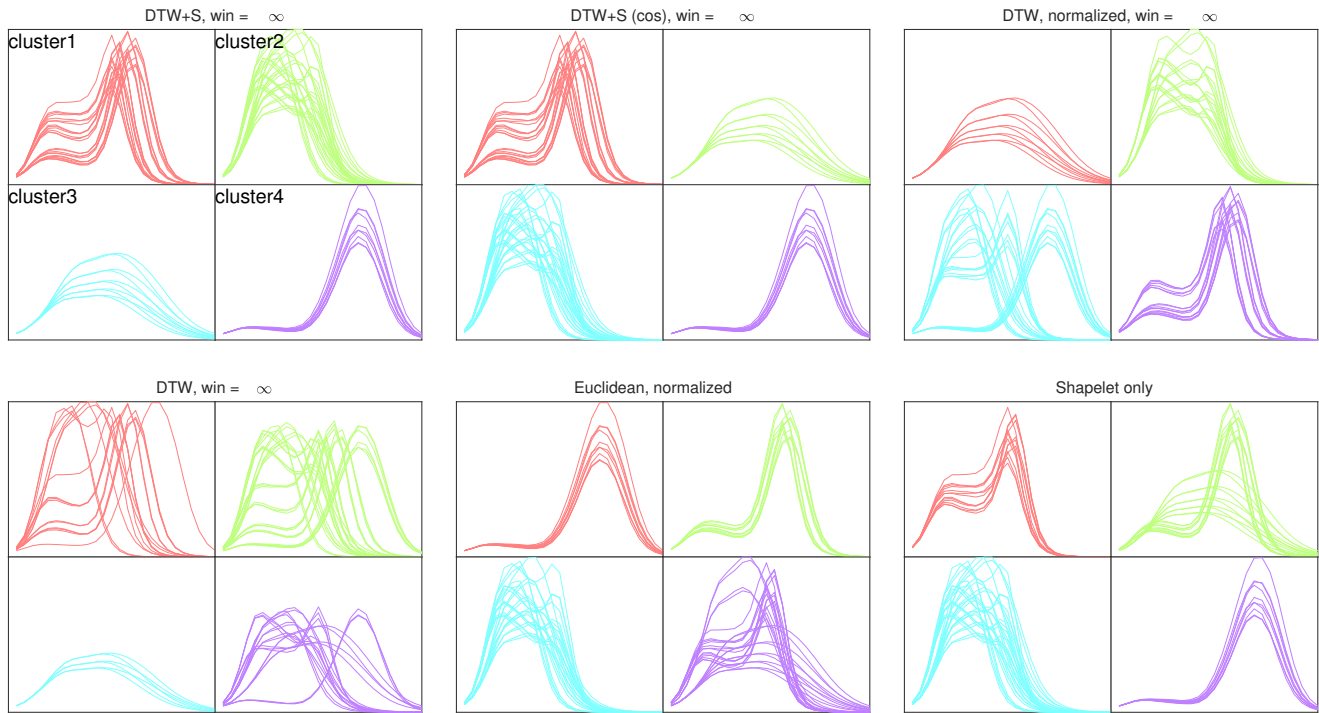


Fig. 5: Comparison of clustering results obtained from DTW+S against other distance measures. DTW+S with Euclidean (default) and cosine distance produces reasonable clustering. All other measures mix different patterns into one cluster.

IV. EXPERIMENTS

We conducted a series of experiments to demonstrate the utility of DTW+S. Specifically, we wish to demonstrate the following: (1) DTW+S results in a more reasonable clustering compared to several other approaches. (2) DTW+S leads to a more reasonable ensemble that captures the scale and timing of events. (3) DTW+S produced better classification results for many classification tasks, outperforming DTW. In all of our experiments, unless stated otherwise, we used the following set of shapelets: (i) ‘increase’: [1, 2, 3, 4], (ii) ‘surge’: [1, 2, 4, 8], (iii) ‘peak’: [1, 2, 2, 1], and (iv) ‘flat’: [0, 0, 0, 0]. According to Theorems 1 and 2, these shapelets satisfy Property 1. These were chosen because they are easily interpretable, particularly in the domain of epidemics. The matrix C_w constructed as in Theorem 1, using this set of shapelets results in $\|C_w^{-1}\| = 13.1$, which is small when multiplied with functions of small ϵ_0, ϵ_1 as in Equation 5. Some other sets of shapelets that satisfy Property 1 were also tried, and their results were not significantly different.

The flatness was calculated by setting $m_0 = 0$, and $\beta = -\ln 0.1/\theta$, where θ is the median of the maximum “absolute” slope of each time-series. Recall that the “absolute” slope for a given window is calculated by averaging successive differences over the window. Choosing β in such a way ensures that a window of time-series with a median “absolute” slope gets a low flatness of 0.1. All the code was written in

MATLAB and is publicly available ¹.

A. Clustering: A Qualitative Evaluation

We consider time-series projections for weekly influenza hospitalization for a US state by a model from Influenza Scenario Modeling Hub [3]. It has 75 time-series, each corresponding to different choices of parameters and initialization. We calculated the dissimilarity matrix (all pair distances) using the following. (1) DTW+S: our method with infinite window for alignment; (2) DTW+S (cos): same as DTW+S, except that cosine distance is used instead of Euclidean for aligning SSRs; (3) DTW, normalized: Applying DTW after normalizing all time-series to zero mean and unit variance – a common normalization technique used with DTW [22]; (4) DTW: DTW without any transformation or normalization; (5) Euclidean, normalized: Euclidean distance without any time warping on standard normal time-series; and (6) Shapelet-only: Euclidean distance on the SSR without any time-warping. For DTW+S, we generate hierarchical clusters with the number of clusters selected using the Silhouette Coefficient as described in Section III-E. We use the same number of clusters for clustering using each of the above dissimilarity measures.

We refrain from a quantitative evaluation as the metric of evaluation would depend on the choice of a distance measure which is what we are evaluating. So, we choose to demonstrate qualitatively. Figure 5 shows the results of clustering from each of the distance measures. We observe that DTW+S

¹https://github.com/scc-usc/DTW_S_apps

produces four clusters with similarly shaped time-series. DTW with standard normalization mixes clusters 1, 2, and 4. The Shapelet-only measure mixes clusters 1 and 3. DTW+S (cos) produces the same clustering (different ordering). DTW without normalization does not produce any discernable pattern in the trends and instead seems to group together those time-series that have similar peaks heights. Euclidean distance with standard normalization mixes clusters 1, 2 and 4. Note that Shapelet transformation is not sufficient to capture similar time-series due to not being flexible across time. On the other hand, DTW with simple standard normalization cannot capture similar trends that occur at different scales. However, when they are combined in DTW+S, they produce reasonable clustering.

B. Ensembling

We consider seven sets of trajectories, including 75 projections from an Influenza model (Set 1), and more than 1000 trajectories from multiple influenza models for six scenarios each (Sets 2-7). We compare the following four approaches for ensembling. (i) Mean ensemble: the most popular ensemble approach that simply averages values at each time-point [2], [4]; (ii) DTW BA: barycenter averaging with DTW; (iii) DTW (z-norm) BA: barycenter averaging with DTW after applying z-normalization to all trajectories; and (iv) DTW+S BA: barycenter averaging with DTW+S. The resulting ensembles for Set 7 are shown in Figure 6. We observe that DTW+S BA produces the highest peak among all ensembles. Mean ensemble and DTW (z-norm) BA produce almost identical results (the green line overlaps with the blue line) and flatten the peak. To quantitatively compare the ensembles, we measure the fractional error of the ensembles in representing the peak timing and the peak size (i.e., the value and the time) at which the peak occurs. The ground truth is obtained by extracting the peak values (and timing) of all trajectories and averaging them. The results are presented in Table I. Note that our approach is the only one that captures the peak timing and size of the underlying trajectories well for all sets.

Figure 7 shows an intermediate step of computing alignments for a subset of trajectories in Set 1. While DTW+S is not specifically designed to identify peaks, we observe that almost all peaks among different time-series are aligned (marked with a pink ‘x’). The circle denotes the centroid, i.e., the ensemble point of these points. Thus, the ensemble is able to provide a better estimate of the average size of the peak.

C. Classification

For classification, we use 64 datasets available at UCR Time Series Classification 2015 Archive [22]. We removed all the datasets where the length of the time-series was more than 800 and the number of training data instances where more than 700, giving us 64 datasets out of 86. For results on the remaining 22 datasets, please see Section IV-C2. Please recall that our objective is not to create the best classifier, but to demonstrate that DTW+S is able to discriminate between time-

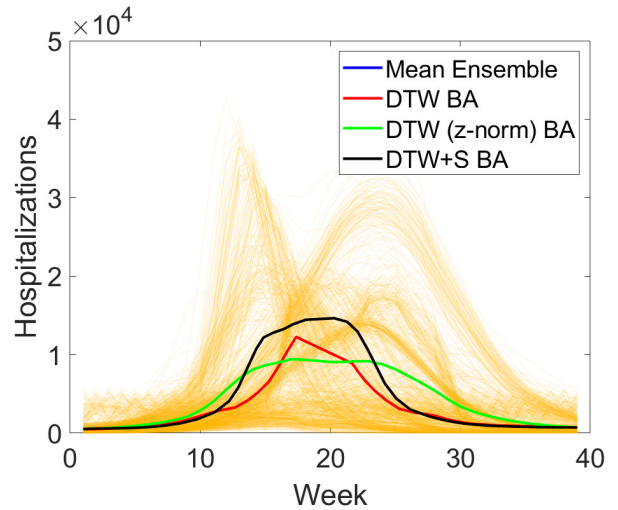


Fig. 6: Results of different ensembling approaches on Set 7. The dark yellow lines represent the individual trajectories.

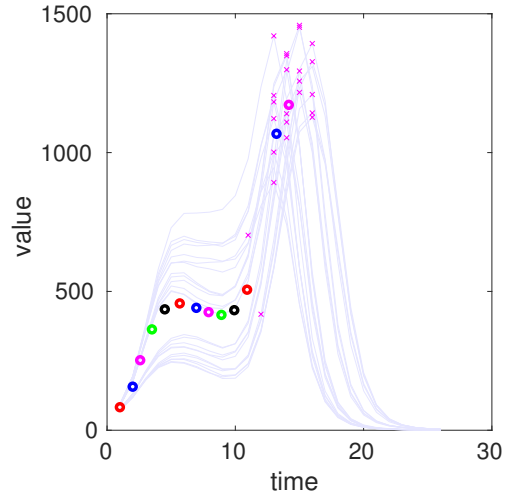


Fig. 7: An instance of alignment, marked by a pink ‘x’ on the individual time-series. The pink circle represents the ensemble point. Previous circles represent the ensemble points obtained from previous alignments.

series of different classes for many datasets and to understand a characterization of such datasets.

For each dataset, we find the 1-nearest neighbor for each instance of test time-series in the training set using DTW+S and assign its class. Then, we evaluate our approach using error defined as the fraction of misclassification, which is the commonly used evaluation method for these datasets [5]. We treat the warping window τ as a hyperparameter. We use leave-one-out cross-validation to identify τ as a fraction of the length of the time-series T from a set of values $\tau = \{0, 0.01T, 0.02T, \dots, 0.07T\}$. We compare our results with the reported best performance of DTW [22]. The results are presented in Figure 8. In the scatter plot, each point

TABLE I: Fractional error in estimation of peak size and timing. Darker red means higher error.

	Method	Mean ensemble	DTW BA	DTW (z-norm) BA	DTW+S BA
Peak Size	Set 1	-0.37	-0.04	-0.01	-0.02
	Set 2	-0.29	-0.33	-0.29	-0.01
	Set 3	-0.38	-0.31	-0.38	-0.03
	Set 4	-0.28	-0.22	-0.28	-0.01
	Set 5	-0.38	-0.23	-0.38	-0.03
	Set 6	-0.28	-0.21	-0.29	-0.02
	Set 7	-0.37	-0.18	-0.37	-0.03
Peak Timing	Set 1	0.08	-0.05	-0.01	0.08
	Set 2	-0.08	-0.10	-0.08	-0.03
	Set 3	-0.15	-0.11	-0.15	0.07
	Set 4	-0.09	-0.08	-0.09	-0.03
	Set 5	0.10	-0.09	-0.10	0.07
	Set 6	-0.09	-0.08	-0.09	-0.02
	Set 7	-0.10	-0.08	-0.10	0.07

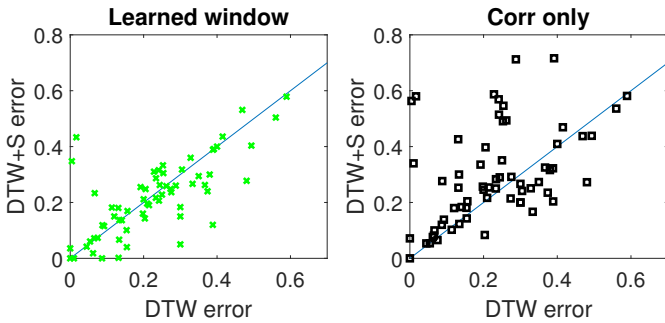


Fig. 8: Performance of DTW+S on 64 datasets.

represents errors on a dataset. The blue line represents the line $y = x$, i.e., when DTW+S has the same error as that of DTW. A point lying below (and to the right) of this line indicates that DTW+S error was lower than DTW error. We observe that DTW+S outperforms DTW on 57.7% datasets. The two measures lead to similar errors for many datasets (along the $y = x$ line). “Corr only” represents the DTW+S measure obtained by ignoring the “flat” shapelet. In this case, DTW+S reduces to the set of Person correlations with the three other shapelets. DTW+S (corr) only outperforms DTW in 39.1% datasets. Additionally, it produces some large errors. Correlation ignores scale completely, and small fluctuations that are not necessarily useful patterns, but noise can cause the measure to consider it similar to some other significant patterns. Thus, the *flatness dimension has a significant contribution* to the performance of DTW+S.

We note that DTW+S does not outperform DTW on all datasets. This is *expected as DTW+S focuses more on the shapes rather than the scale*. Figure 9 shows examples where DTW+S and DTW have significantly different performances. For the dataset in Figure 9a, DTW+S has an error of 0.0017 while DTW has an error of 0.13. This is because DTW+S picks up small local trends (a spike around time 30) present in one class and absent in another class. This is not captured by DTW alone. For the dataset in Figure 9b, DTW+S has an error of 0.23 while DTW has a much lower error of 0.07. For this dataset, the difference in the classes is the scale rather

than the shape in certain parts of the time-series. DTW is able to identify this distinction, making it a less desirable dataset for DTW+S.

1) *Smoothing*: Another type of dataset that would be undesirable for DTW+S is that where the time-series have high noise (Figure 9c). This noise will impact the identification of β for the flatness parameter and the identification of local trends. One way to address this is to smooth the time-series before finding the Shapelet-space Transformation. While a domain expert may choose a reasonable method for smoothing, we use a moving average method with the window size chosen with leave-one-out cross-validation from the set $\{0, 0.1T, 0.2T, 0.4T\}$. The results are shown in Figure 10. The first plot shows that allowing smoothness generally improves the error (many datasets fall to the bottom right). For a very small number of datasets validation results seem to pick a smoothing window that results in worse performance on the test set. In practice, this could be mitigated by having a larger training set. The second plot of Figure 10 shows that the smoothing significantly brings down the error for some datasets (e.g., the three circles on the left of the plot drop close to zero). As an example, the dataset in Figure 9c for which DTW+S was significantly worse (error of 0.35) compared to DTW (0.0044), smoothing results in an error dropping to 0.0022. Finally, the third plot in Figure 10 compares our approach against shapeDTW [13]. We select “HOG1D” version of shapeDTW as it performs the best for this collection of datasets. Without smoothing, there are a few datasets where DTW+S is much worse than shapeDTW (higher in the plot). After smoothing, most datasets accumulate around $y = x$ line.

2) *Results on “Large” Datasets*: In the above analysis, we ignored datasets that were “large”, either because the time-series were long (≥ 700 time steps) or had a large number of training examples (≥ 800). One reason for ignoring large time-series is the computational cost. The complexity of performing 1-NN classification for each test case is $(wT^2|\mathcal{D}_{train}|)$, where $|\mathcal{D}_{train}|$ is the number of time-series in the training set. Second reason is due to difficulty in interpretability. Throughout the paper, we use shapelets of length four, expecting that patterns in four consecutive points form a local trend. In time-series of 1000s of points, with potentially high sampling rates it remains

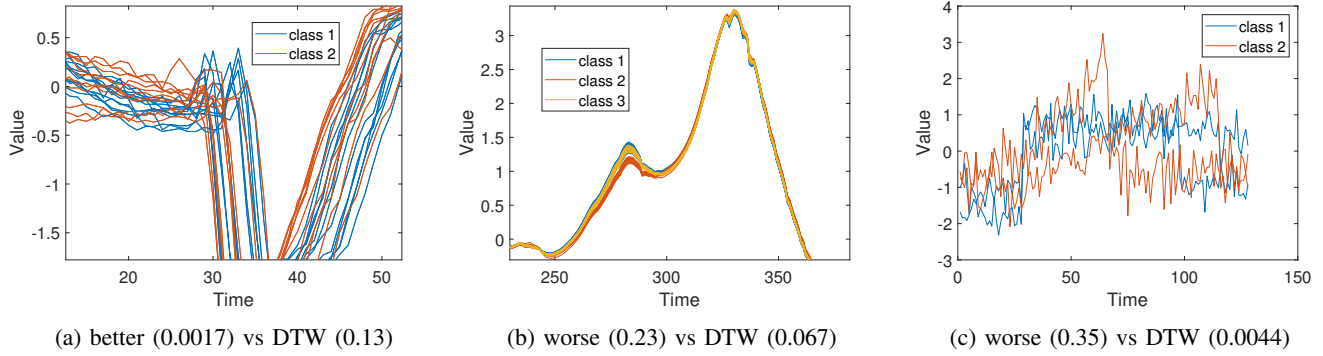


Fig. 9: Section of time-series color-coded to show the different classes. (a) DTW+S picks up small local trends that are not captured by DTW alone. (b) The difference in the classes is the scale rather than the shape in certain parts of the time-series, making it not a desirable dataset for DTW+S. (c) The time-series possess noise preventing DTW+S from identifying trends.

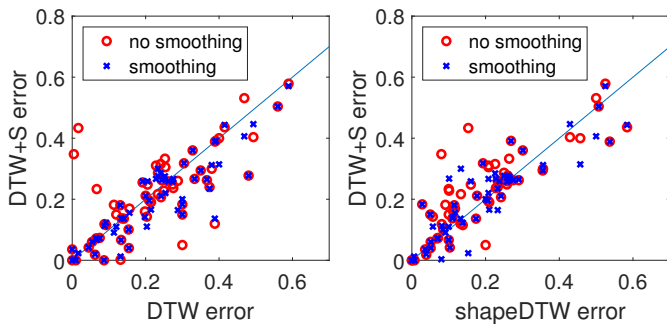


Fig. 10: Results obtained by DTW+S with smoothing. (a) Improvement on many datasets where DTW+S was worse than DTW. (b) Comparison against shapeDTW.

unclear if a set of four points can form a discriminative trend without an in-depth study of the data source. Regardless, we ran experiments on these datasets by sampling – for datasets that were ignored due to the length of the time-series, we sampled every 10th point. For those that were ignored due to having many training instances, we sampled 100 (at regular intervals). We observed that, despite data being sampled, on exactly 50% of the datasets DTW+S outperformed DTW.

V. DISCUSSION

a) Interpretability: A key advantage of our approach is interpretability. Since the SSR is determined by the similarity of the given trend with respect to pre-defined shapes of interest, one can easily make sense of the representation. This is particularly useful for application domains where there exist certain shapes of interest (e.g., increase and peak in public health) and there is resistance towards adopting black-box approaches. Figure 11 shows the SSR of two samples each from two classes of a dataset. This is the dataset corresponding to Figure 9a, where we observed small peaks appearing in one of the classes. Based on the SSR of the samples, we observe that samples for class 1 show a bright yellow (high value) corresponding to dimension 2. On the other hand, samples

from class 2 have a dull yellow (lower value) for the same dimension. This dimension corresponds to the shapelet “peak” = [1, 2, 2, 1], thus suggesting that a peak around the $t = 25$ makes sample 1 in class 1 more similar to sample 2 in class 1 compared to the samples in another class.

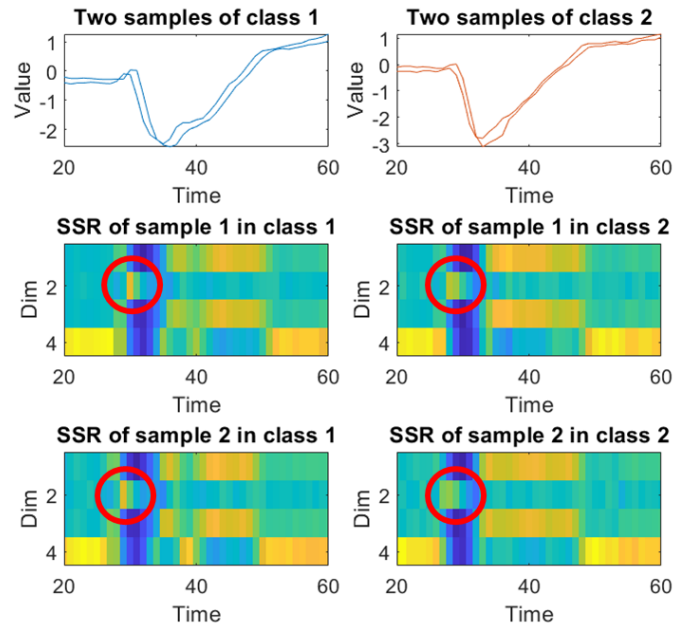


Fig. 11: Interpreting the Shapelet Space Representation.

b) Limitations: Our approach is *not designed for general-purpose classification* or encoding, particularly, where shapes have little impact compared to the scale. Furthermore, while warping windows and smoothing parameters can be set through validation, the best utilization of DTW+S would require some domain knowledge to understand their appropriate setting and the choice of shapelets. However, Theorems 1 and 2 act as guidelines to ensure that the chosen shapelets satisfy the desired property of closeness preservation. Another limitation is the implementation – currently, we use $\mathcal{O}(wT^2)$ time and space for DTW on the distance matrix obtained

from SSR. Here, the T^2 term is contributed by the number of distances to be calculated for a pair of time-series of length T , and w is the number of shapelets. In future work, we will explore existing optimizations of DTW [23] and attempt to transfer them to DTW+S.

VI. CONCLUSION

We have proposed a novel interpretable distance measure for time-series that looks for a sequence of similar trends occurring around the same time. It can capture local trends in a representation that is closeness-preserving. We have demonstrated that our approach DTW+S, which applies DTW on our SSR matrices, results in better clustering, which cannot be achieved by DTW or SSR alone. We have developed an ensemble method using DTW+S that captures both the aggregate scale and timing of the individual time-series significantly better than the currently used mean ensemble and DTW-based barycenter averaging. We have shown that DTW+S can result in better classification compared to other measures for a large number of datasets, particularly those where local trends play a key role.

REFERENCES

- [1] M. Müller, "Dynamic time warping," *Information retrieval for music and motion*, pp. 69–84, 2007.
- [2] US SMH, "COVID-19 Scenario Modeling Hub." <https://github.com/midas-network/covid19-scenario-modeling-hub>, 2020.
- [3] US SMH, "Flu Scenario Modeling Hub." <https://fluscenariomodelinghub.org/>, 2022.
- [4] European CDC, "European COVID-19 Scenario Hub." <https://github.com/covid19-forecast-hub-europe/covid19-scenario-hub-europe>, 2022.
- [5] F. Petitjean, G. Forestier, G. I. Webb, A. E. Nicholson, Y. Chen, and E. Keogh, "Dynamic time warping averaging of time series allows faster and more accurate classification," in *2014 IEEE international conference on data mining*, pp. 470–479, IEEE, 2014.
- [6] A. Srivastava, S. Singh, and F. Lee, "Shape-based evaluation of epidemic forecasts," in *2022 IEEE International Conference on Big Data (Big Data)*, pp. 1701–1710, IEEE, 2022.
- [7] F. Petitjean, A. Ketterlin, and P. Gançarski, "A global averaging method for dynamic time warping, with applications to clustering," *Pattern recognition*, vol. 44, no. 3, pp. 678–693, 2011.
- [8] C. A. Ratanamahatana and E. Keogh, "Making time-series classification more accurate using learned constraints," in *Proceedings of the 2004 SIAM international conference on data mining*, pp. 11–22, SIAM, 2004.
- [9] L. Ye and E. Keogh, "Time series shapelets: a new primitive for data mining," in *Proceedings of the 15th ACM SIGKDD international conference on Knowledge discovery and data mining*, pp. 947–956, 2009.
- [10] Y.-S. Jeong and R. Jayaraman, "Support vector-based algorithms with weighted dynamic time warping kernel function for time series classification," *Knowledge-based systems*, vol. 75, pp. 184–191, 2015.
- [11] J. Lines and A. Bagnall, "Time series classification with ensembles of elastic distance measures," *Data Mining and Knowledge Discovery*, vol. 29, pp. 565–592, 2015.
- [12] E. Dharmo, N. Ismailaja, and E. Kalluçi, "Comparing the efficiency of cid distance and cort coefficient for finding similar subsequences in time series," in *Sixth International Conference ISTI*, pp. 5–6, 2015.
- [13] J. Zhao and L. Itti, "shapedtw: Shape dynamic time warping," *Pattern Recognition*, vol. 74, pp. 171–184, 2018.
- [14] P. J. Van Fleet, *Discrete wavelet transformations: An elementary approach with applications*. John Wiley & Sons, 2019.
- [15] E. Howerton, L. Contamin, L. C. Mullany, M. Qin, N. G. Reich, S. Bents, R. K. Borchering, S.-m. Jung, S. L. Loo, C. P. Smith, *et al.*, "Informing pandemic response in the face of uncertainty. an evaluation of the us covid-19 scenario modeling hub," *medRxiv*, 2023.
- [16] R. Borchering, "Flusight 2023-2024." <https://github.com/cdcepi/FluSight-forecast-hub>, 2023.
- [17] J. Divasón and J. Aransay, "Rank-nullity theorem in linear algebra," *Archive of Formal Proofs*, 2013.
- [18] W. H. Day and H. Edelsbrunner, "Efficient algorithms for agglomerative hierarchical clustering methods," *Journal of classification*, vol. 1, no. 1, pp. 7–24, 1984.
- [19] H. B. Zhou and J. T. Gao, "Automatic method for determining cluster number based on silhouette coefficient," in *Advanced materials research*, vol. 951, pp. 227–230, Trans Tech Publ, 2014.
- [20] A. Mueen, E. Keogh, and N. Young, "Logical-shapelets: an expressive primitive for time series classification," in *Proceedings of the 17th ACM SIGKDD international conference on Knowledge discovery and data mining*, pp. 1154–1162, 2011.
- [21] L. Gupta, D. L. Molfese, R. Tammana, and P. G. Simos, "Nonlinear alignment and averaging for estimating the evoked potential," *IEEE transactions on biomedical engineering*, vol. 43, no. 4, pp. 348–356, 1996.
- [22] Y. Chen, E. Keogh, B. Hu, N. Begum, A. Bagnall, A. Mueen, and G. Batista, "The ucr time series classification archive," July 2015. www.cs.ucr.edu/~eamonn/time_series_data/.
- [23] E. J. Keogh and M. J. Pazzani, "Scaling up dynamic time warping for datamining applications," in *Proceedings of the sixth ACM SIGKDD international conference on Knowledge discovery and data mining*, pp. 285–289, 2000.